# Optical properties of low-temperature grown GaAs on Bragg reflectors

M. Giehler,[a] J. Herfort, W. Ulrici, L. Däweritz, and K. H. Ploog
*Paul-Drude-Institut für Festkörperelektronik, Hausvogteiplatz 5-7, 10117 Berlin, Germany*

(Received 2 January 2002; accepted for publication 18 June 2002)

Near-infrared reflectance spectra of 5 $\mu$m thick low-temperature (LT) GaAs films grown by molecular-beam epitaxy at different substrate temperatures $T_G$ on GaAs/AlAs Bragg reflectors (BR's) have been studied. With decreasing $T_G$ (increasing absorption coefficient $\alpha_f$ of the film), the reflectance of the stop band of the BR decreases monotonously, while the amplitudes of the interference fringes due to the LT-GaAs layer inside the stop band initially increase followed by a decrease for large $\alpha_f$ values. This unusual behavior is explained by a particular optical interference effect of a thick absorbing layer on a strongly reflecting structure. This effect remarkably improves the determination of $\alpha_f$ and enables the detection of As-antisite defects in LT-GaAs films for concentrations as low as $1\times10^{18}$ cm$^{-3}$, where other methods fail. © *2002 American Institute of Physics.* [DOI: 10.1063/1.1499747]

## I. INTRODUCTION

In recent years, low-temperature GaAs (LT GaAs) has been the subject of considerable interest because of its strong nonlinear optical properties combined with short carrier lifetimes.[1,2] These properties are attributed to the large amount of excess As ($\approx$1 at.%), which is incorporated during the growth mainly as As-antisite point defects $As_{Ga}$. A new application is the implementation of LT GaAs for the generation of ultrashort light pulses of Nd:glass fiber lasers operating at 1.06 $\mu$m based on intensity dependent defocusing.[3,4] For this purpose, rather thick (5 to 20 $\mu$m) LT-GaAs layers on a strongly reflecting Bragg reflector (BR) are required. On the one hand, an increasing concentration of As-antisite defects $[As^0_{Ga}]$ in these LT-GaAs layers decreases the desired carrier lifetimes. On the other hand, with increasing $[As^0_{Ga}]$, the undesired broad linear optical absorption in the spectral region above 0.7 eV increases.[5] This absorption is due to transitions from the $As^0_{Ga}$-midgap level into the conduction band in LT GaAs. Therefore, the $[As^0_{Ga}]$ value is an important parameter for the optimization of such devices, which has to be accurately controlled. We have recently demonstrated that reflectance-difference spectroscopy can serve as a tool in order to determine $[As^0_{Ga}]$ during the growth by molecular-beam epitaxy (MBE).[4,6] This method works well for growth at substrate temperatures $T_G$ between 200 °C and 280 °C.[6] However, for layer growth at a substrate temperature $T_G>280$ °C, the optical anisotropy shows only a weak dependence on $T_G$, although $[As^0_{Ga}]$ is expected to change quite drastically.[6] Double-crystal x-ray diffraction (DCXRD) measurements fail for As-antisite defects in LT-GaAs films for concentrations lower than about $10^{19}$ cm$^{-3}$. Finally, a direct estimate of $[As^0_{Ga}]$ using near-infrared absorption spectroscopy also fails, since the stop band of the BR of such devices falls into the spectral range of the broad absorption band of the $As^0_{Ga}$.

We present a method for the determination of $[As^0_{Ga}]$, which uses near-infrared reflection spectroscopy of LT-GaAs layers grown on a BR. We will show that due to a particular optical interference effect, the determination of the absorption coefficient of the LT-GaAs film, $\alpha_f$, is considerably improved and enables the detection of As-antisite defects for concentrations as low as $1\times10^{18}$ cm$^{-3}$, where all other methods fail.

## II. SAMPLES

For the study of the optical properties of LT-GaAs films as well as its suitability for short-pulse laser applications, we have designed and grown a series of 5 $\mu$m thick LT-GaAs layers deposited on top of an GaAs/AlAs BR by MBE. The BR consists of 16 periods with $d_{GaAs}=77.3$ and $d_{AlAs}=91.7$ nm. The thicknesses of the GaAs and the AlAs layers were chosen in order to tune the center frequency of the first stop band close to the operating frequency of the Nd:glass fiber laser at 1.06 $\mu$m. The ratio of the layer thicknesses $d_{GaAs}/d_{AlAs}$ was chosen in order to obtain a maximum for the width of the first stop band, in which the laser emits. The As-antisite point defect density and, hence, the $\alpha_f$ value was varied by changing $T_G$ in the range between 270 °C and 340 °C. These values of $T_G$, which are relatively high for LT GaAs, are a compromise to achieve sufficiently thick layers of good crystalline quality and to retain a sufficient optical nonlinearity and a short carrier lifetime.

## III. EXPERIMENTAL RESULTS

The structural properties of the samples were analyzed by DCXRD rocking curves in the vicinity of the (004) reflection of the GaAs substrate. Figure 1 displays the measured DCXRD rocking curves of the LT-GaAs layers deposited on a BR. The curve for the layer grown at 270 °C shows a peak positioned at 0°, which belongs to the (004) reflection of the GaAs substrate, whereas the one with the highest intensity is attributed to the (004) reflections of the LT-GaAs layer. All other peaks are satellite reflections of the BR with

[a]Electronic mail: giehler@pdi-berlin.de

 

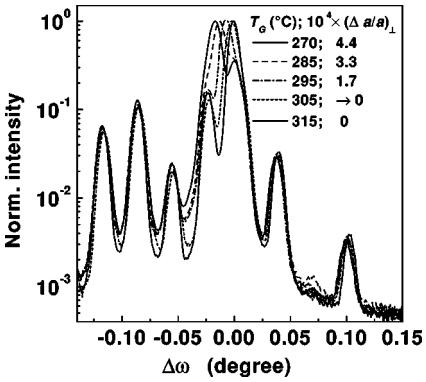


FIG. 1. Semi-logarithmic plot of the normalized intensity of the DCXRD rocking curves for the LT-GaAs layers deposited on a BR at different $T_G$. The $\omega$-axis is normalized with respect to the (004) reflection of the GaAs substrate.

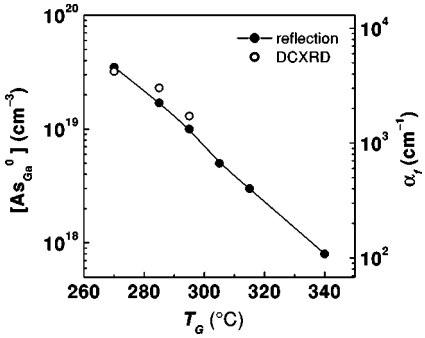


FIG. 3. Concentration of As-antisite defects and absorption coefficient of the LT-GaAs layers at 10 000 cm$^{-1}$ for different films vs $T_G$ determined from reflection (solid dots) and DCXRD measurements (open dots). The DCXRD data refer only to the $[As_{Ga}^0]$ axis.

its zero order peak at $\Delta\omega = -0.088°$. The experimental DCXRD rocking curves of all samples were analyzed using the standard dynamical Takagi–Taupin theory. The agreement between the fits and the experimental results is best, when the perpendicular lattice mismatch between the GaAs substrate and the LT-GaAs layer $(\Delta a/a)_\perp$ was used as a fit parameter. For the thickness of the GaAs/AlAs pairs, we used the nominal values. Figure 1 shows that $(\Delta a/a)_\perp$ decreases with increasing $T_G$ and vanishes for samples with $T_G > 300\,°C$.

The near-infrared reflection spectra were measured with a Bruker Fourier-transform infrared spectrometer IFS 66v at nearly normal incidence and room temperature. The spectra shown in Fig. 2 are plotted from top to bottom for samples with decreasing $T_G$ as indicated in the figure. The spectrum of the BR without the LT-GaAs film (top spectrum) displays the stop band with a reflectance close to one and the side lobes of the BR. The spectra of the samples with LT-GaAs films exhibit additional Fabry–Perot interference fringes inside and outside of the stop band. The reflectance of the plateau of the stop band decreases monotonously with decreasing $T_G$. However, with decreasing $T_G$, the amplitudes of the interference fringes within the stop band (in Fig. 2 denoted by the dashed line *F*) initially increase, but decrease for further decreasing $T_G$. In contrast, the amplitudes of the interference fringes outside of the stop band decrease monotonously.

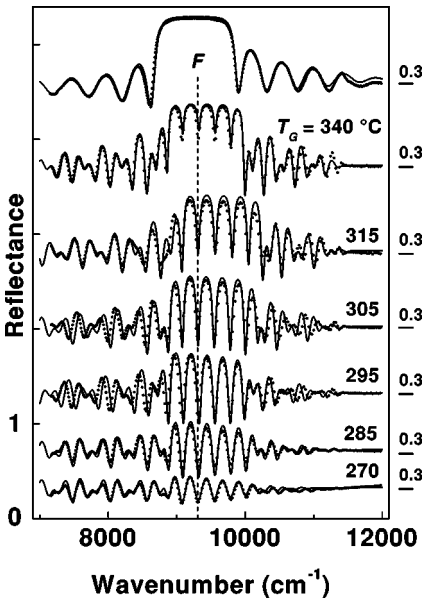


FIG. 2. Measured (dots) and fitted reflection spectra (lines) of LT-GaAs films grown on a GaAs/AlAs BR at different $T_G$ as indicated. The uppermost spectra belongs to a BR without the LT-GaAs layer. The offset of each spectrum is indicated on the right-hand side by the reflectance value of $R = 0.3$.

## IV. MODEL CALCULATIONS AND DISCUSSION

In the following, we analyze the observed spectral features in terms of the linear absorption coefficient of the LT-GaAs film $\alpha_f$. For this purpose, we fit the spectra shown in Fig. 2 by using the transfer-matrix method.[7] In the fit procedure, we take into account the spectral dependence of the dielectric functions of GaAs and AlAs by using the data published in Ref. 8. As fit parameters, we use the period of the GaAs/AlAs pairs of the BR (the thicknesses of the GaAs and AlAs layers were varied according to $\Delta d_{GaAs}/\Delta d_{AlAs} = \text{const.}$), the thickness of the LT-GaAs film $d_f$, and the concentration of the $As_{Ga}^0$ defects, which determines the strength of the EL2-like absorption. We have obtained the EL2-like absorption spectrum from the measurement of a semi-insulating GaAs sample with As-antisite defects, in which the $[As_{Ga}^0]$ concentration was determined according to Ref. 9. Finally, in the simulations, we have carried out a spectral averaging over the intensities of all partial waves within the substrate,[10] in order to prevent interference fringes in the calculated spectra due to the substrate in agreement with the experimental findings. The fitted spectra shown in Fig. 2 are in excellent agreement with the measured ones. We would like to point out that the layer thicknesses $(d_{GaAs}, d_{AlAs}, d_f)$ obtained from the fitting procedure also agree within less than 1% with the nominal values.

Next, we compare the concentration of As-antisite defects determined by the proposed reflection method with the data from the DCXRD measurements. Figure 3 shows $[As_{Ga}^0]$ and $\alpha_f$ for all samples obtained from analyzing their reflection spectra. The $[As_{Ga}^0]$ values change by almost two

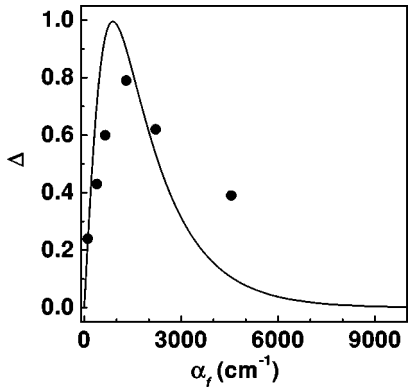


FIG. 4. Experimentally determined values (dots) and calculated data (line) of $\Delta$ for the interference fringe $F$ in Fig. 2 for different LT-GaAs films indicated by the absorption coefficient $\alpha_f$.

orders of magnitude within this narrow range of $T_G$ and can be detected for concentrations as low as $1\times10^{18}$ cm$^{-3}$. For comparison, we have included in Fig. 3 also the $[As^0_{Ga}]$ data determined from the DCXRD rocking curves using the calibration factor given in Ref. 11. For $T_G<300\,^\circ$C, both values agree very well with each other. For $T_G>300\,^\circ$C, however, the DCXRD method fails, since $[As^0_{Ga}]$ is too small to change $(\Delta a/a)_\perp$. Therefore, our reflection method provides the only possibility to determine $[As^0_{Ga}]$ for LT-GaAs layers on a strongly reflecting medium over a large concentration range.

The sensitivity of the reflection method is based on two effects, which are clearly observable in Fig. 2. First, with decreasing $T_G$ (increasing $\alpha_f$ and $[As^0_{Ga}]$), the reflectance of the stop band of the BR monotonously decreases. Second, with decreasing $T_G$, the amplitudes of the interference fringes of the LT-GaAs film within the stop band of the BR (denoted by the dashed line $F$ in Fig. 2) initially increase up to $T_G\approx300\,^\circ$C, but decrease with a further lowering of $T_G$. In Fig. 4, the experimentally determined amplitudes $\Delta$ of these interference fringes are plotted versus $\alpha_f$, where $\Delta=(R^{\max}-R^{\min})/(R^{\max}+R^{\min})$ and $R^{\max}$ ($R^{\min}$) denote the reflectance data at the maximum (minimum) of the interference dip $F$ in Fig. 2. The dependence of $\Delta$ on $\alpha_f$ shown in Fig. 4 is anomalous. Normally, in the case of weakly reflecting substrates, $\Delta$ decrease monotonously with increasing $\alpha_f$ according to $\Delta\propto e^{-2\alpha}$. The particular optical property of a thick absorbing film on a strongly reflecting substrate remarkably enhances the accuracy of the fit procedure and therewith the detection limit of the As-antisite defects in the LT-GaAs films.

If we approximate the strong reflectance of the LT-GaAs film/BR interface, $R_{fm}$, within the stop band of the BR by $R_{fm}=|r_{fm}|^2\approx1$, we obtain

$$\Delta\approx\frac{2r\,e^{-2\Phi}(r^2-1)(1-e^{-4\Phi})}{(r^2+e^{-4\Phi})(1+r^2\,e^{-4\Phi})-4r^2\,e^{-4\Phi}},\qquad(1)$$

where $r$ denotes the real part of the reflection coefficient of the air/film interface (the imaginary part was neglected) and $\Phi$ the imaginary part of the phase shift in the layer, e.g., $\Phi\sim\alpha_f$. The line in Fig. 4 shows the calculated results for $\Delta$ using Eq. (1). In this calculation, we have approximated, without loss of generality, the strong reflectance of the stop band of the BR by the reflectance of an Al mirror (with the dielectric constant $\varepsilon_{Al}=-90+i26$).[8] The simulated dependence of $\Delta$ versus $\alpha_f$ qualitatively follows the measured one. Differences between the calculated and the measured data occur due to the approximations used in Eq. (1). These approximations are necessary in order to get a more comprehensive equation than it is obtained by the full analytical calculation of the transfer matrix. For $\alpha_f\to0$, the reflectance of an air/film/mirror structure is determined by the strong reflectance of the film/mirror interface, $R^{\max,\min}\approx1$, therefore $\Delta\approx0$ (cf. Fig. 4). In the case of constructive interference between the partial waves propagating from the air/film and film/mirror interfaces, $R^{\max}$ decreases monotonously with increasing $\alpha_f$, because the constructive superposition is suppressed. However, in the case of destructive interference, backward and forward propagating waves have opposite phases. For $r+e^{-2\Phi}=0$, the attenuated partial waves returning from the strongly reflecting film/metal interface cancel exactly the partial waves propagating forward from the air/film interface and we obtain $R^{\min}=0$, which gives the maximum $\Delta\approx1$ at about $\alpha_f=1000$ cm$^{-1}$ (cf. Fig. 4). With further increasing $\alpha_f$, the amplitude of the partial waves propagating backward from the film/mirror interface decreases, and these waves can no longer cancel the waves from the air/film interface so that $R^{\min}$ increases and $\Delta$ decreases. Therefore, the strong reflectance of the film/mirror interface in the case of destructive superposition is the crucial point for the unusual behavior of $\Delta$ versus $\alpha_f$.

## ACKNOWLEDGMENTS

The authors would like to thank H. T. Grahn for helpful discussions.

[1] See, e. g., J. F. Whitaker, Mater. Sci. Eng., B **22**, 61 (1993).
[2] M. R. Melloch, J. M. Woodall, E. S Harmon, N. Otsuka, F. H. Pollak, D. D. Nolte, R. M. Feenstra, and M. A. Lutz, in *Annual Review of Material Science*, edited by B. W. Wessels, E. N. Kaufmann, J. A. Giodmaine, and J. B. Wachtman, Jr. (Palo Alto, 1995), Vol. 25, p. 547.
[3] M. Leitner, P. Glas, T. Sandrock, M. Wrage, G. Apostopoulos, H. Kostial, J. Herfort, K.-J. Friedland, and L. Däweritz, Opt. Lett. **24**, 1567 (1999).
[4] J. Herfort, G. Apostopoulos, W. Ulrici, K.-J. Friedland, H. Kostial, L. Däweritz, M. Leitner, P. Glas, and K. H. Ploog, Jpn. J. Appl. Phys., Part 1 **39**, 2452 (2000).
[5] M. O. Manasreh, D. C. Look, K. R. Evans, and C. E. Stutz, Phys. Rev. B **41**, 10272 (1990).
[6] G. Apostolopoulos, J. Herfort, W. Ulrici, L. Däweritz, and K. H. Ploog, Phys. Rev. B **60**, R5145 (1999).
[7] P. Yeh, *Optical Waves in Layered Media* (Wiley, New York, 1988), p. 102.
[8] D. Y. Smith, E. Shiles, M. Inokuti, and E. D. Palik, in *Handbook of Optical Constants of Solids, Part I*, edited by E. D. Palik (Academic, New York, 1985), pp. 369 and 429; *ibid. Part II* (Academic, New York, 1991), p. 489.
[9] P. Silverberg, P. Omling, and L. Samuelson, Appl. Phys. Lett. **52**, 1689 (1988).
[10] B. Harbeke, Appl. Phys. B: Photophys. Laser Chem. **39**, 165 (1986).
[11] X. Liu, A. Prasad, J. Nishio, E. R. Weber, Z. Lilliental-Weber, and W. Walukiewicz, Appl. Phys. Lett. **67**, 279 (1995).